GEOPHYSICS, VOL. XXXI, NO. 3 (JUNE, 1966), PP. 524–535, 7 FIGS

SYNTHETIC SEISMOGRAMS OF *P* WAVES PROPAGATING IN SOLID WEDGES WITH FREE BOUNDARIES†

KARL FUCHS*

A numerical method for the synthesis of seismograms for body wave propagation in solid wedges is presented. The method is based on the superposition of multiple reflections arising from the entrance of a plane primary wave. Therefore the method is restricted to that part of the time domain where no diffracted waves from the wedge axis occur. In spite of this restriction, dispersion of body waves in wedges can well be studied by this method.

Seismograms have been synthesized which show the dispersion of a primary *p*-signal propagating in a solid 10-degree and a 5-degree wedge with free boundaries. For wedge angles less than 10 degrees the signal front (to be distinguished from the wavefront) suddenly decreases its velocity from that in the infinite medium to about that of the plate wave as the signal approaches the wedge axis. Simultaneously in this transition zone a decrease of the dominant period of the interference signal occurs. These observations are concordant with previous model studies.

Particle motion diagrams disclose elliptical polarization of the interference signal in the neighborhood of the wedge axis; the polarization changes its sense from prograde to retrograde on passing through the transition zone.

1. INTRODUCTION

Wave propagation in elastic layers with plane parallel boundaries has been investigated thoroughly both in experiments and in theory. However, plane parallel interfaces are not the rule but rather the exception within the earth's crust. Usually the interfaces are not parallel, but form angles less than 10 degrees. These are the wedge-shaped media. While the plate with free boundaries is the prototype of the layered medium with plane parallel interfaces, the wedge with free boundaries may be regarded as the prototype of the layered medium with nonparallel interfaces.

Most of the work on wave propagation in a wedge has been concerned with surface waves of the Rayleigh and Love type, with their transmission and reflection at the wedge axis. The propagation of body waves in wedges has received comparatively little attention. Hudson (1963) obtained the solution for *SH* waves from a line source in a wedge. This corresponds to the case of acoustic waves propagating in a liquid or gaseous wedge since no converted waves arise in this problem. Complete solutions for the case of *P* or *SV* wave propagation have not reached the author's attention.

In a recent paper (Fuchs, 1965) the author investigated the propagation of body waves in solid wedges with free boundaries by two-dimensional model experiments. To compare the experimental results with theory a simplified method of computing synthetic seismograms for the propagation of body waves in a wedge was proposed. This method was limited up to the time when the primary wave, traveling inside the wedge, reached the axis of the wedge and gave rise to diffracted waves. Limited computer facilities allowed only the computation of synthetic seismograms down to wedge angles of 10 degrees.

In this paper the time scope of the proposed method will be extended. Synthetic seismograms for propagation of body waves inside a 10-degree and a 5-degree wedge will be presented. These synthetic seismograms are concordant with the author's earlier model observations. Particle motion diagrams reveal the presence of elliptical polarization near the wedge axis not so far observed in model experiments.

After outlining the proposed method in section 2, certain features of propagation of *P* waves in a wedge, especially signal velocity and polarization, will be discussed in section 3 with the help of synthetic seismograms.

2. METHOD OF SYNTHESIZING SEISMOGRAMS FOR *p*-WAVE PROPAGATION INSIDE A WEDGE WITH FREE BOUNDARIES

Outline of the method

Figure 1 explains the terms used in the description of the wedge and the coordinate system. The

† Manuscript received by the Editor July 26, 1965.

* Saint Louis University, St. Louis, Missouri. Now with Geophysikalisches Institut, Technische Hochschule Karlsruhe-West, Germany.

wedge is bounded by its two faces, which intersect at the wedge axis, forming the wedge angle 2α. The median plane bisects the wedge angle. We shall only consider two-dimensional wave propagation with planes of equal phases parallel to the wedge axis. Therefore the process can be described in the right handed $x-y$ system as depicted in Figure 1.

The wedge medium will be characterized by the velocity a of p waves:

$$a = \sqrt{\frac{\lambda + 2\mu}{\rho}} \tag{1}$$

and the velocity b of s-waves:

$$b = \sqrt{\frac{\mu}{\rho}} \tag{2}$$

where λ and μ are Lame's constants and ρ the density of the medium. The velocity a' of the so-called plate-wave is given by:

$$a' = \sqrt{\frac{4\mu(\lambda + \mu)}{\rho(\lambda + 2\mu)}} \cdot \tag{3}$$

The quotient Q of the p- and s-wave velocity is:

$$Q = \frac{a}{b} \cdot \tag{4}$$

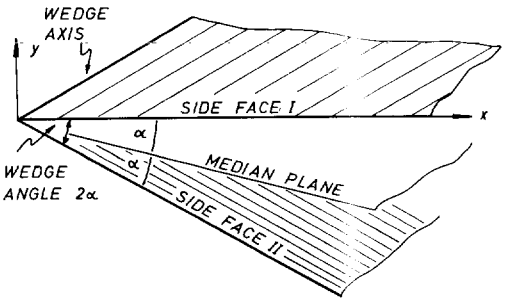

FIG. 1. Wedge geometry.

Other terms will be explained where they appear in this paper.

To obtain a first idea on dispersion of body waves propagating in a solid wedge we shall consider the propagation of a plane dilatational (p) signal. Such a wave will be considered to propagate from the open end of the wedge towards its axis in the direction of the median plane with wavefront parallel to the wedge axis.

The primary p-signal is followed by a tail of multiple reflections of both p- and s-type as indicated in Figure 2. The number of multiple reflections will increase considerably as the wedge angle becomes smaller. At large distances from the wedge axis these reflections are well separated from one another; but, as the primary signal is approaching the wedge axis, reflections start to interfere with the primary signal and among themselves. Therefore a deformation of the

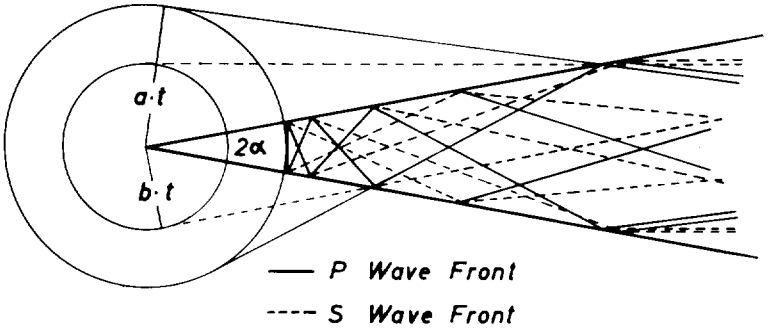

FIG. 2. Construction of multiple reflections in a solid wedge. Case of $2\alpha = 15°$.

primary signal is to be expected. The question is whether this interference of multiple reflections can account for some features of body wave propagation observed in wedges or expected from wave propagation in plates. For the synthesis, we shall sum up the effect of all multiple reflections inside a solid wedge due to the entrance of a plane primary p signal, so that the boundary conditions on the side faces are automatically satisfied. This method determines the total effect at all points inside the wedge up to the time of arrival of the diffracted wave generated at the wedge axis. The solutions are valid at a point of distance, r, from the wedge axis up to the time t_d after the arrival of the primary front at the axis where

$$t_d = \frac{r}{a}. \tag{5}$$

If we restrict our synthesis up to this time we can construct exact solutions. In the next section, we will give some basic formulas needed for the computation of multiple reflections. Then the response of the wedge to an arbitrary shape of the primary signal will be analytically derived from the response to an impulse.

Basic formulas for multiple reflections in a wedge

We shall derive the horizontal and vertical displacement components u and v from the displacement potentials $\phi(t, x, y)$ and $\psi(t, x, y)$ by:

$$u = \frac{\partial \phi}{\partial x} - \frac{\partial \psi}{\partial y}, \tag{6}$$

$$v = \frac{\partial \phi}{\partial y} + \frac{\partial \psi}{\partial x}. \tag{7}$$

Let a plane P signal be incident on the side face of a solid wedge at an angle of incidence $\gamma_{p\nu}$. Let the corresponding displacement potential have the general form:

$$\phi_{i\nu}(t, x, y) = P\left(t + \frac{x}{a}\sin\gamma_{p\nu} - \frac{y}{a}\cos\gamma_{p\nu}\right). \tag{8}$$

Then a p wave is reflected at the same angle $\gamma_{p\nu}$ and with some amplitude $r_{11\nu}$ with the displacement potential:

$$\phi_{r\nu}(t, x, y) = r_{11\nu}P\left(t + \frac{x}{a}\sin\gamma_{p\nu} + \frac{y}{a}\cos\gamma_{p\nu}\right). \tag{9}$$

An s wave is reflected at the angle $\gamma_{s\nu}$ and the amplitude $r_{12\nu}$ with the displacement potential:

$$\psi_{r\nu}(t, x, y) = r_{12\nu}P\left(t + \frac{x}{b}\sin\gamma_{s\nu} + \frac{y}{b}\cos\gamma_{s\nu}\right). \tag{10}$$

Correspondingly, at the incidence of a plane s-signal at the angle $\gamma_{s\nu}$ on the side face of the wedge with the displacement potential:

$$\psi_{i\nu}(t, x, y) = P\left(t + \frac{x}{b}\sin\gamma_{s\nu} - \frac{y}{b}\cos\gamma_{s\nu}\right) \tag{11}$$

there is generated a reflected s-wave at the same angle $\gamma_{s\nu}$ and amplitude $r_{22\nu}$ with displacement potential:

$$\psi_{r\nu}(t, x, y) = r_{22\nu}P\left(t + \frac{x}{b}\sin\gamma_{s\nu} + \frac{y}{b}\cos\gamma_{s\nu}\right) \tag{12}$$

and a reflected p wave under the angle $\gamma_{p\nu}$ and amplitude $r_{21\nu}$ with displacement potential:

$$\phi_{r\nu}(t, x, y) = r_{21\nu}P\left(t + \frac{x}{a}\sin\gamma_{p\nu} + \frac{y}{a}\cos\gamma_{p\nu}\right). \tag{13}$$

In these expressions $\gamma_{p\nu}$ and $\gamma_{s\nu}$ are related by Snell's law:

$$\frac{\sin\gamma_{p\nu}}{a} = \frac{\sin\gamma_{s\nu}}{b}, \tag{14}$$

and $r_{11\nu}$, $r_{12\nu}$, $r_{21\nu}$, $r_{22\nu}$ are the well-known reflection coefficients for plane waves incident on the free surface of a half-space. For reference their analytical expressions are given for arbitrary ratio Q of p- and s wave velocity (see equation (4)):

$$r_{11\nu} = \frac{4 \cot \gamma_{p\nu} \cot \gamma_{s\nu} - [Q^2 \cot^2 \gamma_{p\nu} + (Q^2 - 2)]^2}{4 \cot \gamma_{p\nu} \cot \gamma_{s\nu} + [Q^2 \cot^2 \gamma_{p\nu} + (Q^2 - 2)]^2} \tag{15}$$

$$r_{12\nu} = -\frac{4 \cot \gamma_{p\nu}[Q^2 \cot^2 \gamma_{p\nu} + (Q^2 - 2)]}{4 \cot \gamma_{p\nu} \cot \gamma_{s\nu} + [Q^2 \cot^2 \gamma_{p\nu} + (Q^2 - 2)]^2} \tag{16}$$

$$r_{21\nu} = \frac{4 \cot \gamma_{s\nu}[Q^2 \cot^2 \gamma_{p\nu} + (Q^2 - 2)]}{4 \cot \gamma_{p\nu} \cot \gamma_{s\nu} + [Q^2 \cot^2 \gamma_{p\nu} + (Q^2 - 2)]^2} \tag{17}$$

and

$$r_{22\nu} = r_{11\nu}. \tag{18}$$

It can be remarked from equations (8) through (13) that the primary p wave and all the reflected p waves have, except for a multiplying factor, the displacement potential:

$$P\left(t + \frac{x}{a} \sin \gamma_{p\nu} \pm \frac{y}{a} \cos \gamma_{p\nu}\right). \tag{19}$$

Correspondingly all the s waves generated by the primary p wave and its reflections have, except for a factor, the displacement potential:

$$P\left(t + \frac{x}{b} \sin \gamma_{s\nu} \pm \frac{y}{b} \cos \gamma_{s\nu}\right). \tag{20}$$

Therefore if a p wave has a front:

$$t + \frac{x}{a} \sin \gamma_{p\nu} \pm \frac{y}{a} \cos \gamma_{p\nu} = 0, \tag{21}$$

then the fronts of the corresponding s waves are:

$$t + \frac{x}{b} \sin \gamma_{s\nu} \pm \frac{y}{b} \cos \gamma_{s\nu} = 0, \tag{22}$$

and vice versa. From equations (21) and (22), one realizes that all the p fronts are tangents to the circle with radius at about the wedge axis, and that all the s-fronts form tangents to the circle with radius bt about the same axis. Here t is the time the primary front (and all secondary wave fronts) need to arrive at the axis. This has been indicated in Figure 2. The connection of the wavefronts at the side faces together with their being tangents to the two circles provides an easy method of constructing the multiple reflections in the wedge.

The response of the wedge to an arbitrary signal derived from the response to an impulse

We shall now set up the formulas for the displacements caused by the primary or the multiple reflections on the side face $I(y=0)$ of the wedge. The restriction to displacements on the side face does not mean that the described method is not applicable to points inside the wedge. The side face I has only been chosen to compare the resulting synthetic seismograms directly with the model observations carried out on the side face of the wedge (Fuchs, 1965). For later generalization to arbitrary shape of the primary signal we shall start with a unit step form for the displacement potential ϕ_{i1}:

$$\phi_{i1}(t, x, y) = U\left(t + \frac{x}{a} \sin \gamma_{p1} - \frac{y}{a} \cos \gamma_{p1}\right) \tag{23}$$

where U is the Heaviside unit step function with

$$\frac{\partial U(z)}{\partial z} = \delta(z), \tag{24}$$

and $\delta(z)$ is the well-known Dirac delta function with

$$\delta(z) = 0 \quad \text{for } z \neq 0, \tag{25}$$

and $\delta(0)$ goes to infinity such that:

$$\int_{-\infty}^{+\infty} \delta(z)\, dz = 1. \tag{26}$$

Therefore the displacement due to the primary wave has the form of a δ-function. The sum of all reflections derived from the primary δ-signal will be termed the δ-response of the wedge. From this δ-response we can easily calculate the response to an arbitrary signal by convolution. According to

equations (8) and (9), the primary p signal from (23) gives rise to a reflected wave with displacement potential:

$$\phi_{r1}=r_{111}l'\left(t+\frac{x}{a}\sin\gamma_{p1}+\frac{y}{a}\cos\gamma_{p1}\right) \quad (27)$$

and a reflected s wave with displacement potential (equation (10)):

$$\psi_{r1}=r_{121}l'\left(t+\frac{x}{a}\sin\gamma_{p1}+\frac{y}{b}\cos\gamma_{s1}\right). \quad (28)$$

From the total displacement potentials:

$$\phi_1=\phi_{i1}+\phi_{r1} \quad (29)$$

and

$$\psi_1=\psi_{r1} \quad (30)$$

the x-component $u(t, x, y)$ and the y-component $v(t, x, y)$ of the displacement are derived according to equations (6) and (7) on the side face $I(y=0)$ of the wedge:

$$u_1=\frac{1}{a}\left[(1+r_{111})\sin\gamma_{p1}-\frac{a}{b}r_{121}\cos\gamma_{s1}\right]\delta(z_1) \quad (31)$$

$$v_1=\frac{1}{a}\left[-(1-r_{111})\cos\gamma_{p1}+r_{121}\sin\gamma_{p1}\right]\delta(z_1) \quad (32)$$

where

$$z_1=\left(t+\frac{x}{a}\sin\gamma_{p1}\right). \quad (33)$$

More generally, if a p-signal, resulting from the primary signal by multiple reflections, is incident on the side face $I(y=0)$ with angle $\gamma_{p\nu}$, one finds that it gives rise to a resultant horizontal displacement $u_\nu(t, x, 0)$ and a resultant vertical displacement $v_\nu(t, x, 0)$:

$$u_\nu(t, x, 0)=G_{u\nu}R_{p\nu}\delta(z_\nu) \quad (34)$$

$$v_\nu(t, x, 0)=G_{v\nu}R_{p\nu}\delta(z_\nu) \quad (35)$$

where

$$G_{u\nu}=\frac{1}{a}\left[(1+r_{11\nu})\sin\gamma_{p\nu}-\frac{a}{b}r_{12\nu}\cos\gamma_{s\nu}\right] \quad (36)$$

and

$$G_{v\nu}=\frac{1}{a}\left[-(1-r_{11\nu})\cos\gamma_{p\nu}+r_{12\nu}\sin\gamma_{p\nu}\right]. \quad (37)$$

Accordingly an s-signal, resulting from the primary signal by multiple reflections and incident on the side face I with angle $\gamma_{s\mu}$ gives rise to a resultant horizontal displacement $u_\mu(t, x, 0)$ and a resultant vertical displacement $v_\mu(t, x, 0)$ on side face I:

$$u_\mu(t, x, 0)=G_{u\mu}R_{s\mu}\delta(z_\mu) \quad (38)$$

$$v_\mu(t, x, 0)=G_{v\mu}R_{s\mu}\delta(z_\mu) \quad (39)$$

where

$$G_{u\mu}=\frac{1}{a}\left[r_{21\mu}\sin\gamma_{p\mu}+\frac{a}{b}(1-r_{22\mu})\cos\gamma_{s\mu}\right], \quad (40)$$

and

$$G_{v\mu}=\frac{1}{a}\left[r_{21\mu}\cos\gamma_{p\mu}+(1+r_{22\mu})\sin\gamma_{p\mu}\right]. \quad (41)$$

R_{pi} and R_{si} in equations (34), (35) and (38), (39) are the reduction factors of the incident waves which result from amplitude reduction due to multiple reflections of the respective waves (e.g. *psp*, *pspps*, etc.). These reduction factors are the products of the corresponding reflection coefficients. The symbols z_ν and z_μ stand for:

$$z_l=t+\frac{x}{a}\sin\gamma_{pl} \qquad l=\nu, \mu \quad (42)$$

Until the arrival of the diffracted wave at distance x a total of m_p p-reflections and of m_s s-reflections might contribute to the displacements on the side face I. Thus the resultant signal for the horizontal displacement $u_\delta(t, x, 0)$ due to a primary δ-signal is:

$$u_\delta(t, x, 0)=\sum_{\nu=1}^{m_p}u_\nu(t, x, 0)+\sum_{\mu=1}^{m_s}u_\mu(t, x, 0) \quad (43)$$

and the resultant vertical displacement $v_\delta(t, x, 0)$ is:

$$v_\delta(t, x, 0) = \sum_{\nu=1}^{m_p} v_\nu(t, x, 0) + \sum_{\mu=1}^{m_s} v_\mu(t, x, 0). \tag{44}$$

For wedge angles less than 20° the computation of the reflection coefficients and the reflection angles, as well as $G_{u\nu}$, $G_{v\nu}$, $G_{u\mu}$, $G_{v\mu}$ in equations (36), (37), (40), and (41) should be done by digital computers.

The horizontal and vertical δ-responses of the wedge on its side face are $u_\delta(t, x, 0)$ and $v_\delta(t, x, 0)$. The responses to an arbitrary signal shape $f(t)$ are obtained by convolution:

$$u(t, x, 0) = \int_{-\infty}^{+\infty} u_\delta(\bar{t}, x, 0) f(t - \bar{t})\, d\bar{t} \tag{45}$$

$$v(t, x, 0) = \int_{-\infty}^{+\infty} v_\delta(\bar{t}, x, 0) f(t - \bar{t})\, d\bar{t}. \tag{46}$$

With equations (43), (44) this can be written as:

$$u(t, x, 0) = \sum_{\nu=1}^{m_p} \int_{-\infty}^{+\infty} u_\nu(\bar{t}, x, 0) f(t - \bar{t})\, d\bar{t} + \sum_{\mu=1}^{m_s} \int_{-\infty}^{+\infty} u_\mu(\bar{t}, x, 0) f(t - \bar{t})\, d\bar{t} \tag{47}$$

$$v(t, x, 0) = \sum_{\nu=1}^{m_p} \int_{-\infty}^{+\infty} v_\nu(\bar{t}, x, 0) f(t - \bar{t})\, d\bar{t} + \sum_{\mu=1}^{m_s} \int_{-\infty}^{+\infty} v_\mu(\bar{t}, x, 0) f(t - \bar{t})\, d\bar{t}. \tag{48}$$

Since with $l = \nu, \mu$:

$$\int_{-\infty}^{+\infty} \delta\left(\bar{t} + \frac{x}{a} \sin \gamma_{pl}\right) f(t - \bar{t})\, d\bar{t} = f\left(t + \frac{x}{a} \sin \gamma_{pl}\right) \tag{49}$$

we find finally for the horizontal and vertical response to an arbitrary shaped primary signal (see equations (34), (35), (38), (39))

$$u(t, x, 0) = \sum_{\nu=1}^{m_p} G_{u\nu} R_{p\nu} f\left(t + \frac{x}{a} \sin \gamma_{p\nu}\right) + \sum_{\mu=1}^{m_s} G_{u\mu} R_{s\mu} f\left(t + \frac{x}{a} \sin \gamma_{p\mu}\right) \tag{50}$$

and

$$v(t, x, 0) = \sum_{\nu=1}^{m_p} G_{v\nu} R_{p\nu} f\left(t + \frac{x}{a} \sin \gamma_{p\nu}\right) + \sum_{\mu=1}^{m_s} G_{v\mu} R_{s\mu} f\left(t + \frac{x}{a} \sin \gamma_{p\mu}\right). \tag{51}$$

The number m_p of p- and m_s of s-reflections in the wedge of angle 2α is dependent on the wedge angle 2α, on the angle of incidence γ_{p1} of the primary signal and on the ratio Q of p-wave to s-wave velocity. In the case of the solid wedge it is not possible to give explicit formulas for m_p and m_s; but neither is it necessary to have advance knowledge of m_p or m_s. The scheme of constructing multiple reflections as indicated in Figure 2 will also be followed in the computer program. For the iteration procedure the following points should be noted:

a) We will use amplitude 1 and angle of incidence $\gamma_{p1} = 90° - \alpha$ for the primary p wave. This means symmetrical propagation with respect to the median plane of the wedge. By this the computer work will be reduced drastically.

b) Every p-wave with amplitude $R_{p\nu}$ incident on one side face at angle $\gamma_{p\nu}$ will cause a reflected pp-wave with angle $\gamma_{p\nu}$ and amplitude:

$$R_{p\nu+1} = r_{11\nu} R_{p\nu} \tag{52}$$

and a reflected ps-wave with angle

$$\gamma_{s\nu} = \arcsin \frac{b}{a} \sin \gamma_{p\nu} \tag{53}$$

and amplitude:

$$R_{s\nu+1} = r_{12} R_{p\nu}. \tag{54}$$

c) On the opposite face of the wedge the pp-reflection will be incident with:

$$\gamma_{p\nu+1} = \gamma_{p\nu} - 2\alpha \tag{55}$$

and the ps-reflection with:

$$\gamma_{s\nu+1} = \gamma_{s\nu} - 2\alpha. \tag{56}$$

d) Correspondingly the amplitudes and angles of incidence for the sp- and ss-type of reflec-

tions arising from an incident s-wave can be calculated.

e) Once the angle of incidence for a p- or s-reflection is known, the arrival time of the wave at a certain point $P(x,0)$ on the face I can be computed from equation (21) or (22)

$$t = -\frac{x}{a}\sin\gamma_p = -\frac{x}{b}\sin\gamma_{sv}. \quad (57)$$

f) The program for the computation of the amplitudes and angles of incidence for all multiple reflections consists essentially of a subprogram which generates for any given incident p- or s-wave either the two reflections of the pp- or ps-type, or of the sp- and ss-type. The output of the subprogram contains information on the angle of incidence of the new wave, its amplitude and its type. The output is fed through a memory device back into the input so that the subprogram might give birth to a new generation of reflections, again of either pp, ps or sp, ss-type.

g) As soon as the angle γ_p or γ_s becomes negative in the operation described under (c) and (d), we are dealing with a reflection returning out of the wedge. Now the operations (55) and (56) increase the absolute angles of incidence.

h) All returning reflections for which an angle

$$|\gamma_p| \geq 90° \quad (58)$$

or

$$|\gamma_s| \geq \arcsin\frac{b}{a} \quad (59)$$

has been calculated, are not continued to the opposite side face of the wedge as plane waves, but are linked to diffracted waves arising at the wedge axis. The subprogram will not produce new returning reflections for which (58) or (59) is fulfilled. Thus we limit our solution to all waves arriving at a given point before the set of diffracted waves from the wedge axis.

i) The number of reflections for a finite wedge angle is finite. Yet this number increases considerably as the wedge angle decreases. For instance, for the 15-degree wedge and $(a/b)^2=3$ about 250 reflections have to be summed up. The number increases for the 10-degree wedge to about 2,600 reflections. In case of the 5-degree wedge, over 60,000 reflections are estimated. Thus for small angles this method can only be handled by computers with large memory capacity. In the case of the 5-degree wedge the synthetic seismograms were computed only up to time $t=0$, the arrival of the primary wavefront at the wedge axis. Even then, 2,200 reflections had to be summed.

The program for the calculation of angles of incidence and of amplitudes for the multiple reflections has been written in Fortran II for an IBM 7072. The output of this program represents the δ-response of the wedge on its face both for vertical and horizontal components.

A second program in Fortran II for an IBM 7072 convolves this δ-response with any desired function $f(t)$. This $f(t)$ can be thought of as either:

a) the original shape of the primary signal,
b) the δ-response of a receiver system, or
c) the response of the receiver system to the primary signal as input.

3. FEATURES OF BODY WAVE PROPAGATION IN A WEDGE DISCUSSED FROM SYNTHETIC SEISMOGRAMS

The method outlined in the previous section has been used to compute synthetic seismograms for the cases of solid 10-degree and 5-degree wedges with free boundaries and $Q=\sqrt{3}$ (i.e. Poisson's constant $\sigma=0.25$). As the primary signal, a Gaussian pulse has been used:

$$f(t) = \frac{1}{\sqrt{\tau}}\exp\left[-\pi\left(\frac{t}{\tau}\right)^2\right] \quad (60)$$

which has a Fourier transform:

$$c(\nu) = \int_{-\infty}^{+\infty} f(t)\exp\left[-2\pi\nu t i\right]dt$$
$$= \exp\left[-\pi\tau^2\nu^2\right]. \quad (61)$$

Following Brillouin (1962) we define the effective duration of our signal $f(t)$ as:

$$\Theta = \frac{1}{f(0)}\int_{-\infty}^{+\infty}|f(t)|\,dt \quad (62)$$

and the effective band width, of its spectrum as:

$$2\nu_1 = \frac{1}{c(0)} \int_{-\infty}^{+\infty} |\, c(\nu) \,|\, d\nu. \qquad (63)$$

The signal $f(t)$ has been chosen in such a way that according to (62) the effective duration is:

$$\Theta = \tau \qquad (64)$$

and the effective band width:

$$2\nu_1 = \frac{1}{\tau} \cdot \qquad (65)$$

It is advantageous to use a nondimensional time T:

$$T = \frac{t}{\tau} \cdot \qquad (66)$$

This is equivalent to the use of a primary signal of unit duration ($\tau = 1$) and unit bandwidth ($2\nu_1 = 1$):

$$f(T) = \exp(-\pi T^2), \qquad (67)$$

and

$$c(\nu) = \exp(-\pi\nu^2). \qquad (68)$$

In the numerical computation we shall approximate the actual Gaussian pulse by:

$$\bar{f}(T) = \begin{cases} 0 & \text{for } |T| > 1 \\ \exp(-\pi T^2) & \text{for } |T| \leq 1, \end{cases} \qquad (69)$$

and shall introduce a time shift $T_0 = 1$ into the signal, so that the beginning of $\bar{f}(T)$ is now at $T = 0$:

$$\bar{f}(T) = \begin{cases} 0 \quad \text{for } |T-1| > 1 \\ \exp[-\pi(T-1)^2] \\ \qquad \text{for } |T-1| \leq 1. \end{cases} \qquad (70)$$

The signal actually used for the convolution is $\bar{f}(T)$. The signal starts with a small discontinuity of about 5 percent of its maximal amplitude. The same jump occurs at the end of the signal at $T = 2$.

The distance from the wedge axis will also be measured in nondimensional units:

$$\Delta = \frac{x}{a\tau} = \frac{x}{L} \qquad (71)$$

where

$$L = a\tau \qquad (72)$$

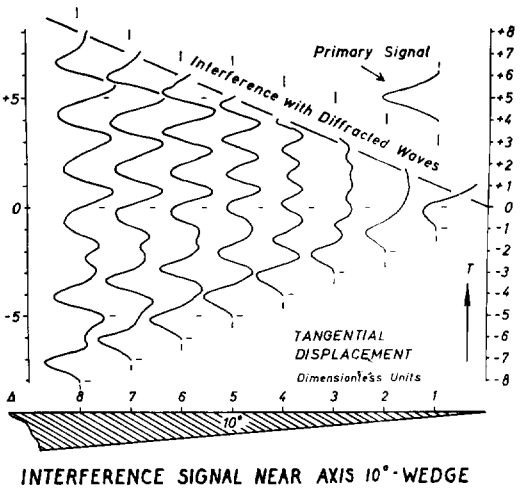

FIG. 3. Interference signal near the axis of 10 degree wedge with free boundaries (Poisson's constant $\sigma = 0.25$). Tangential displacement on the side face 1 of the wedge. T = time before arrival of wavefront at wedge axis; Δ = distance from wedge axis (dimensionless units).

is the length of the primary signal in space corresponding to its duration τ in time.

Synthetic seismograms for body waves near the axis of 10-degree and 5-degree wedges with free boundaries.

Figures 3 to 5 are examples for synthetic seismograms near the axis of the 10-degree and 5-degree wedges.

Figure 3 displays synthetic seismograms for the tangential (horizontal) displacement on the face near the axis of a 10-degree wedge ($Q = \sqrt{3}$; i.e. $\sigma = 0.25$) with free boundaries. The primary signal is moving into the wedge from left to right towards the wedge axis. The nondimensional distance Δ is measured from the wedge axis. This should not be confused with the distance from the shotpoint. The nondimensional time T is plotted on the vertical scale. $T = 0$ is the time where the theoretical front of the primary wave arrives at the wedge axis $\Delta = 0$. For comparison the primary signal has been included in the figure with the same amplitude scale. As indicated in the figure, the interference signal does not end at the upper ends of the seismograms. From there on, interference with the diffracted waves generated at the wedge axis starts. This part cannot be synthesized by the present method. Attention should be drawn to the following features:

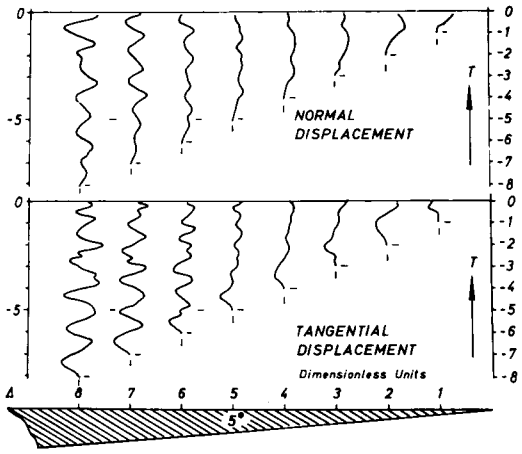

FIG. 4. Interference signal near the axis of a 5-degree wedge with free boundaries (Poisson's constant $\sigma = 0.25$). Normal and tangential displacement on the side face of the wedge (see Figure 3).

a) At the distance $\Delta = 8$ (corresponding to 8 times the length of the primary signal) all reflections interfere. One can no longer separate one reflection from the other. The primary, pulse-shaped signal has been converted into a more or less sinusoidal wave train.

b) Comparison with the primary signal shows that the amplitude does not increase in the synthesized part close to the wedge axis.

c) It is clearly to be noted that the higher frequencies suddenly vanish at about $\Delta = 3$. From here on, a very low frequency becomes apparent. The dominant period rather abruptly doubles.

d) Note also the flattening of the signal onset close to the wedge axis.

Synthetic seismograms for the displacements on the side face of a 5-degree wedge are presented in Figure 4. The same distance range from the wedge axis is considered. For comparison both normal (vertical) and tangential (horizontal) displacements have been depicted. The primary signal moves again from left to right towards the wedge axis. Essentially the same phenomena are to be observed as in Figure 3 for the 10-degree wedge. Especially noteworthy is the stronger flattening of the signal onset close to the axis. This effect is much more pronounced than for the 10-degree wedge.

In Figure 5, a closer look is taken at the beginning of the interference signal for the 5-degree wedge. The figure presents an enlarged portion of the beginnings of the seismograms in Figure 4. The time scale has been reduced with the velocity a of the p-wave in such a manner that in the reduced time scale the theoretical front of the signal arrives at $T_{red} = 0$ for all distances Δ from the axis.

The wavefront is a mathematical abstraction. In practical situations, we are never actually able

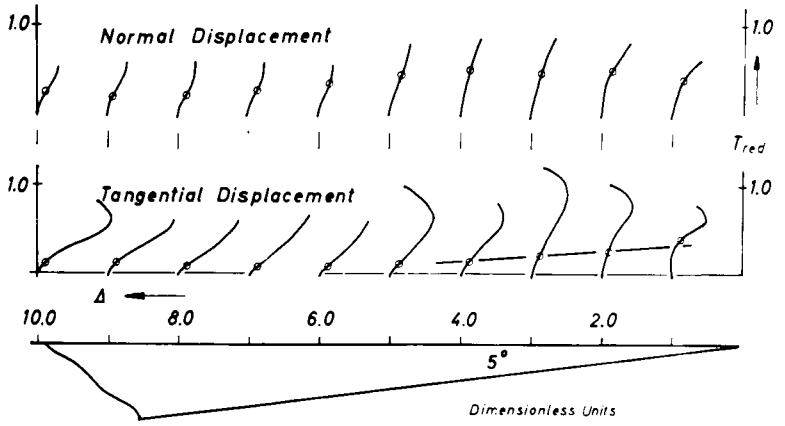

FIG. 5. Velocity of signal front near the axis of a 5-degree wedge. Reduced time scale: $T_{red} = T + \Delta/a$.

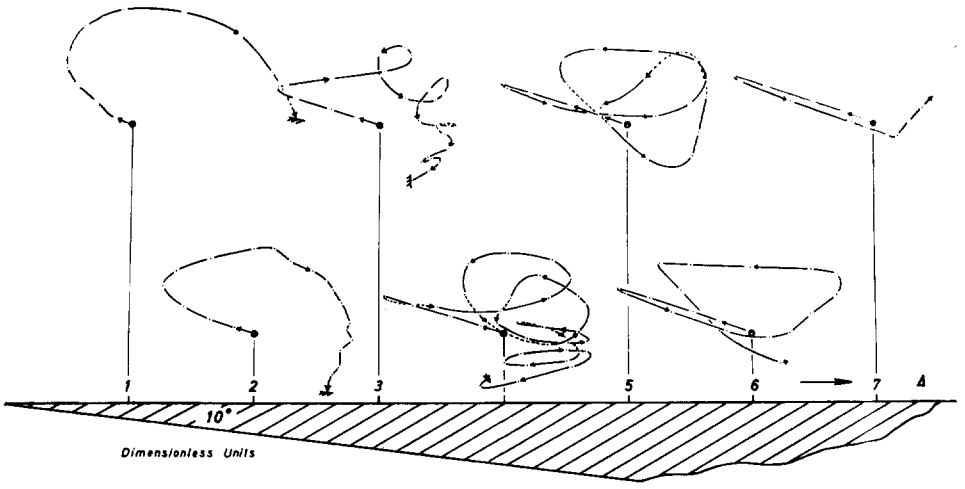

FIG. 6. Particle motion on the side face near the axis of a 10-degree wedge.

to measure the arrival time of the wavefront. Our signal can only be observed embedded in noise (microseisms, recorder noise, interference with other phases, thickness of the trace). Therefore we can only decide that a signal has arrived if a reliable deflection from the zero position and above the noise level is discernible on the recording instrument. We could define this moment as the arrival time of the *signal front* in contrast to the arrival of the theoretical but *not detectable wavefront*. As long as the signal is not dispersed the signal front follows the wavefront at a constant time lag. Thus the measured signal front velocity will not differ from the wavefront velocity. But in case of a dispersed signal, wave front and signal front velocity, in general, do not have the same value and need to be distinguished (see Sommerfeld and Brillouin, 1914; Brillouin, 1960).

The strong flattening of the signal onset in Figure 5 indicates the difference between these two velocities. As stated before, the signal front cannot be defined as sharply as the wavefront, since the signal front depends on the setting of the level at which a reliable reading of a signal arrival can be made. For experimental sake we have arbitrarily chosen this level of reliable reading to be at 1/20 of the maximum amplitude of the primary signal. We have indicated the beginning of the signal, i.e. the signal front, by the circles on the traces of Figure 5. From 10 to about 6 units distance, the signal front follows the wavefront with a constant time lag. From about 5 to 1 unit distances, the signal front is propagating at a speed v_{sig} of about 96 percent of the velocity a of the p-wave:

$$v_{sig} \approx 0.96a. \tag{73}$$

This value comes very close to the velocity a' of the so-called plate wave (equation (3)) for which one derives from equation (1) for $\sigma = 0.25$, i.e. $\lambda = \mu$:

$$a' = 0.943a. \tag{74}$$

It should be mentioned that decreasing the level of reliability to 1/40 of the maximum amplitude of the primary signal only very slightly increases the velocity v_{sig} near the wedge axis, leaving it still significantly below that of the p-wave.

Considering a plane parallel plate as a wedge in the limiting case of vanishing wedge angle 2α, we might conclude that the velocity a' of the plate wave is not a wavefront velocity but the velocity of a signal front.

These observations about signal velocity are concordant with the author's previous measurement of signal velocities in two dimensional wedge shaped models (Fuchs, 1965).

Particle motion diagrams

Particle motion diagrams on the face of the wedge close to the axis were investigated. Dia-

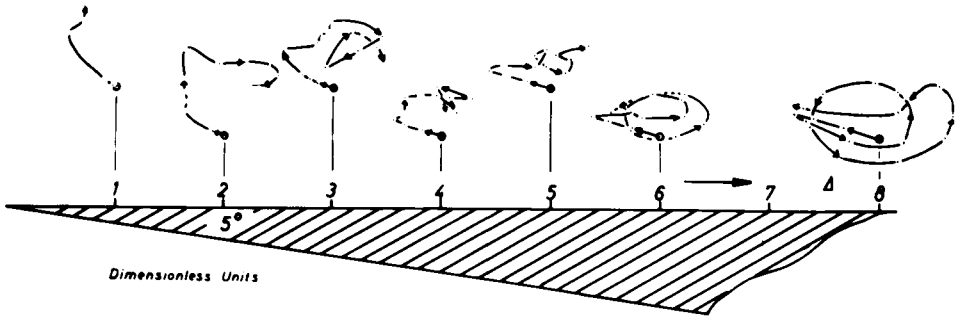

FIG. 7. Particle motion on the side face near the axis of a 5-degree wedge.

grams for the 10-degree and 5-degree wedges are presented in Figures 6 and 7. As before the primary signal is propagating towards the wedge axis (in these figures from right to left). In case of the 10-degree wedge, the particle motion is plotted at different distances Δ from the wedge axis from the time of arrival of the wavefront until the time when the first diffracted wave is expected to arrive.

In case of the 5-degree wedge the motion was only followed until $T=0$, the arrival of the primary signal at the wedge axis.

These particle motion diagrams reveal a rather unexpected feature of p-wave propagation in a wedge. Normal and tangential components most of the time have a phase difference of nearly 90 degrees resulting in elliptical polarization. At larger distances the motion is prograde, at smaller distances it changes to retrograde, resembling the motion of a Rayleigh-type surface wave.

It is remarkable that the change in the sense of the polarization occurs at just the same distance from the wedge axis at which the change in signal velocity and the decrease in dominant frequency occurs. We can therefore speak of a transition zone in the neighborhood of the wedge axis where characteristic features of wave propagation suffer changes:

1) The signal velocity changes from the velocity a of the p-wave to a value close to the velocity a' of the plate wave.
2) The sense of the polarization switches from prograde to retrograde.
3) The dominant frequency of the interference signal decreases significantly.

From the particle motion diagrams, one can estimate the length of that zone to about one unit distance, that is about one wavelength. The transition zone occurs

a) for the 10-degree wedge between about $\Delta=3$ to 4,
b) for the 5-degree wedge between about $\Delta=4.5$ to 5.5.

If we compare the width,

$$2H = 2\Delta \sin \alpha, \tag{75}$$

of the wedge at distance Δ in the transition zone to the length $L=aT=1$ of the primary signal, we find that the transition occurs in case of

a) the 10-degree wedge for $2H/L$ between 0.5 and 0.7,
b) the 5-degree wedge for $2H/L$ between 0.4 and 0.5.

It must be pointed out that the distance of the transition zone from the wedge axis, as derived from the synthetic seismograms, is about two to three times larger than might be estimated by the formula

$$2H/\lambda \approx 0.064,$$

which was derived from the author's model experiments; λ refers to the dominant wavelength of the signal. This dominant wavelength has been estimated by equating the time difference between the first arrival and the first extremum of the measured interference signal to one-fourth of the dominant period of the signal. Using this definition, we derive from the synthetic seismograms

for the ratio $2H/\lambda$ in the transition zone:

a) for the 10° wedge $2H/\lambda \approx 0.2$,
b) for the 5° wedge $2H/\lambda \approx 0.1$.

Since the conditions in the model experiments and the numerical experiments of this paper (source distance, primary signal, two-dimensional model, level of reliability) are not the same, it is hard to determine what might be the cause of this discrepancy.

4. DISCUSSION AND CONCLUSIONS

A relatively simple method of synthesizing seismograms for the propagation of body waves in a solid wedge with free boundaries has been presented. It has been shown that, even in the case of a wedge, important conclusions about the dispersion of body waves can be drawn on the basis of ray theory as long as the solution is restricted to the domain outside the occurrence of diffracted waves.

The synthetic seismograms revealed features of propagation of body waves inside a wedge which are concordant with the author's model experiments in the following points:

1) For wedge angles less than 10 degrees, a decrease of the signal front velocity is to be observed in the neighborhood of the wedge axis.
2) The velocity changes from the velocity of the *p*-wave to about that of the plate wave.
3) The change occurs rather suddenly in a zone, the dimension of which is of the order of the wavelength.
4) While passing through the transition zone the dominant frequency of the signal is abruptly decreased.

The synthetic seismograms allowed the construction of particle motion diagrams which showed elliptical polarization close to the wedge axis. As an additional characteristic of the transition zone a change from prograde to retrograde polarization takes place on the passage of the wave through that zone towards the wedge axis.

In future model and field experiments special care should be taken to verify this polarization by recording vertical and horizontal components. The change of polarization in addition to the decrease in signal velocity and dominant frequency could turn out to be a very valuable means of identifying and exploring wedge-shaped structures of small wedge angles. Finally, it should be pointed out that the same simple method of superposing multiple reflections can and will be used for the investigation of wave propagation in more complicated wedge-shaped structures.

ACKNOWLEDGMENTS

The author is indebted to his colleagues in the Department of Geophysics of Saint Louis University, especially Dr. Carl Kisslinger and the Rev. William Stauder, S.J., for fruitful discussions and their encouraging interest in this work. The research reported in this paper was sponsored by the Air Force Office of Scientific Research, Grant AF-AFOSR 386-63, as part of the Advanced Research Projects Agency's VELA-UNIFORM program. Computing facilities were made available by Washington University, St. Louis, through NSF Grant G-22296.

REFERENCES

Brillouin, L., 1960, Wave propagation and group velocity: New York, Academic Press, 154 p.
——— 1962, Science and information theory (2nd Edit.), New York, Academic Press, 351 p.
Fuchs, K., 1965, Investigation on the wave propagation in wedge-shaped media: Ztschr. f. Geophys., Jhrg. 31, p. 51–89.
Hudson, J. A., 1963, *SH* waves in a wedge-shaped media: Geophys. Journ., v. 7, p. 517–546.
Sommerfeld, A., and Brillouin, L., 1914, Ueber die Fortpflanzung des Lichtes in dispergierenden Medien: Ann. d. Phys., v. 44, p. 177–240.